Annals of Nuclear Medicine Vol. 14, No. 4, 255–261, 2000

# Relationship between cancer cell proliferation and thallium-201 uptake in lung cancer

Masatoshi ISHIBASHI,* Teruhiko FUJII,** Hideaki YAMANA,** Kiminori FUJIMOTO,* Toru RIKIMARU,*** Akihiro HAYASHI,** Seiji KURATA* and Naofumi HAYABUCHI*

*Division of Nuclear Medicine and Department of Radiology,
**Department of Surgery, and ***First Department of Internal Medicine and Respiratory Unit,
Kurume University School of Medicine

Although thallium-201 ($^{201}$Tl) uptake is related to perfusion in many normal tissues, the biologic rationale for $^{201}$Tl uptake in tumors is uncertain. To determine if tumor uptake is related to cell proliferation, we correlated the relative retention of $^{201}$Tl in lung tumors with expression of Ki-67, an indicator of cell proliferation. ***Methods:*** Sixty patients with lung tumors, included small cell carcinoma (n = 8) and non-small cell carcinoma (n = 52), underwent $^{201}$Tl single photon emission computed tomography (SPECT) imaging. The $^{201}$Tl lesion uptake was determined on early and delayed images and the radiotracer retention index (RI) was calculated. Tumor specimens were obtained at surgery or bronchoscopy. The cell proliferation ratio was estimated with MIB-1, a monoclonal antibody that recognized the nuclear antigen Ki-67. ***Results:*** The average $^{201}$Tl index was $2.13 \pm 0.61$ (early) and $2.46 \pm 0.83$ (delayed). The average RI was $17.44 \pm 35.01$. Overall, the $^{201}$Tl index (delayed) and the cancer cell proliferation were correlated ($r = 0.70$, $p < 0.0001$). Of interest, there was a significant correlation ($r = 0.872$, $p < 0.0005$) between the $^{201}$Tl index on delayed images and the cell proliferation ratio in patients with small cell but not non-small cell lung carcinoma. The $^{201}$Tl index (delayed) was significantly higher ($p < 0.0001$) in patients with small cell lung carcinoma than in patients with non-small cell lung carcinoma. ***Conclusion:*** $^{201}$Tl imaging appears to be useful for evaluating patients with small cell lung carcinoma but not non-small lung carcinoma, and is correlated with the monoclonal antibody MIB-1, a marker of cell proliferation.

**Key words:** lung neoplasm, $^{201}$Tl, cell cycle, monoclonal antibody MIB-1, cancer cell proliferation

## INTRODUCTION

LUNG CANCER is a leading cause of death, and although the incidence has been declining modestly in men, it has shown a progressive increase in women. Identification of lung cancer is usually accomplished on chest radiograph or computed tomography (CT) of the chest. Radionuclide imaging with thallium-201 ($^{201}$Tl) has also been advocated to distinguish benign from malignant lesions[1–4] and to identify lymph node metastasis.[5] The radionuclide method has not found wide clinical application, possibly because the correlates of tumor biology and $^{201}$Tl uptake remain poorly defined. Several studies suggest a correlation between uptake and membrane potential,[6–10] but this is more likely an indicator of retention than initial uptake. Other authors suggested a relationship to tumor viability.[5] We sought to determine whether $^{201}$Tl uptake could be used to evaluate the rate of tumor cell proliferation, an important indicator of the genetic behavior of tumors.[11–14] We compared $^{201}$Tl uptake with the number of tumor cells that were positive for the monoclonal antibody MIB-1, a marker of cell proliferation, in patients with lung carcinoma.

Received December 15, 1999, revision accepted May 10, 2000.

For reprint contact: Masatoshi Ishibashi, M.D., Division of Nuclear Medicine and Department of Radiology, Kurume University School of Medicine, 67 Asahi-machi, Kurume, Fukuoka 830–0011, JAPAN.

E-mail: ishi@kurume.ktarn.or.jp

## MATERIALS AND METHODS

*Study Design*

Sixty patients referred for evaluation of a lung mass or nodule between September 1994 and September 1998, who had a diagnosis of lung cancer confirmed by histopathology and who had MIB-1 staining of their tissues were enrolled in this study. Two physicians blinded to the patient's clinical status and to the results of other imaging studies interpreted each imaging study. Staging was based on the TNM classification.[15] There were 50 men and 10 women, ranging in age from 35 to 85 years (mean: 67.4 years). Patients underwent surgery or chemotherapy within 2 weeks after imaging. Informed consent for participation in the study was obtained from each patient or guardian as part of the protocol approved by the Institutional Clinical Subpanel on Human Studies at our university hospital.

*Imaging Protocol*

CT scans were performed with ProSeed (GE Yokogawa Medical Systems, Tokyo, Japan) and X-Vigor (Toshiba, Tokyo, Japan) systems. Images were obtained with 10-mm collimation, at 10-mm intervals, in the supine position, from the lung apices to the adrenal glands. The scanning parameters (120 kVp, 170 to 200 mA, a 1-second scanning time, 30 to 35 cm field of view with a 512 × 512 matrix) varied slightly, depending on the patient's size. Images were printed with settings for mediastinal and lung display. An intravenous bolus injection of 100 mL of the non-ionic contrast medium Iopamidol (300 mg I/m*l*; Bracco Industria Chemica, Milan, Italy) was used.

$^{201}$Tl SPECT and planar images were acquired 20 min and 3 hours after radiotracer (148 MBq) injection. Images were acquired with a large field-of-view, dual detector camera and computer system (RC2600I and RW3000, Hitachi, Tokyo, Japan), equipped with a low-energy, high resolution parallel-hole collimator. The dual detector camera was rotated over 180 degrees in a circular orbit. Images were acquired in 64 steps over 360 degrees of rotation at the rate of 30 sec/view. Data were collected digitally (64 × 64) in a dedicated computer system. Energy discrimination was provided by a 20% window centered on the 68 keV mercury x-ray of $^{201}$Tl. Continuous transaxial tomograms were reconstructed after filtered backprojection with a Butterworth filter to reduce statistical noise (cutoff frequency: 0.22 cycles/pixel, order 8). Coronal and sagittal tomograms of 1 pixel thickness then were reconstructed from the transaxial images. $^{201}$Tl images were obtained within 1 week after CT imaging in all patients.

*Image Interpretation*

CT scans were interpreted prospectively from film by two observers (K.F. and M.I.) blinded to the patients' clinical status and pathologic and $^{201}$Tl studies. The size of the primary lesion and any additional findings (e.g., mediastinal invasion, pleural invasion, postobstructive atelectasis, or pneumonia) were noted, and the final reading was approved by consensus. All hilar and mediastinal lymph nodes larger than 10 mm (short axis) were recorded with the American Thoracic Society (ATS) nodal locations.[15] The TNM staging system of the American Joint Committee on Cancer (AJCC) was used.[16]

**Table 1** Primary lung cancer in 60 patients examined with Tl-201 SPECT

| Classification | | No. of patients |
|---|---|---|
| Non-small cell carcinoma | | 52 |
| Adenocarcinoma | 26 | |
| Squamous cell carcinoma | 23 | |
| Large cell carcinoma | 1 | |
| Adenosquamous carcinoma | 2 | |
| Small cell carcinoma | | 8 |

**Table 2** Clinical and pathologic stage in lung cancer patients (n = 60)

| Classification | | | No. of patients |
|---|---|---|---|
| Non-small cell carcinoma | cStage | I | 5 |
| | | IIIa | 5 |
| | | IIIb | 4 |
| | | IV | 2 |
| | pStage | I | 26 |
| | | II | 2 |
| | | IIIa | 8 |
| Small cell carcinoma | cStage | IIIa | 2 |
| | | IIIb | 2 |
| | | IV | 4 |

Note: No., number; cStage, clinical stage; pStage, pathologic stage

**Table 3** Tl-201 index on early and delayed images and retention index in 60 patients with primary lung cancer

| Classification | Early Tl-201 index | Delayed Tl-201 index | Retention index |
|---|---|---|---|
| Non-small cell carcinoma (n = 52) | 2.07 ± 0.62 | 2.28 ± 0.64 | 13.95 ± 31.92 |
| Small cell carcinoma (n = 8) | 2.58 ± 0.63 | 3.69 ± 0.86 | 41.21 ± 45.41 |
| | | * | |
| Total | 2.13 ± 0.61 | 2.46 ± 0.83 | 17.44 ± 35.01 |

Note: Data are expressed as mean ± sd. unpaired t-test. *: $p < 0.005$

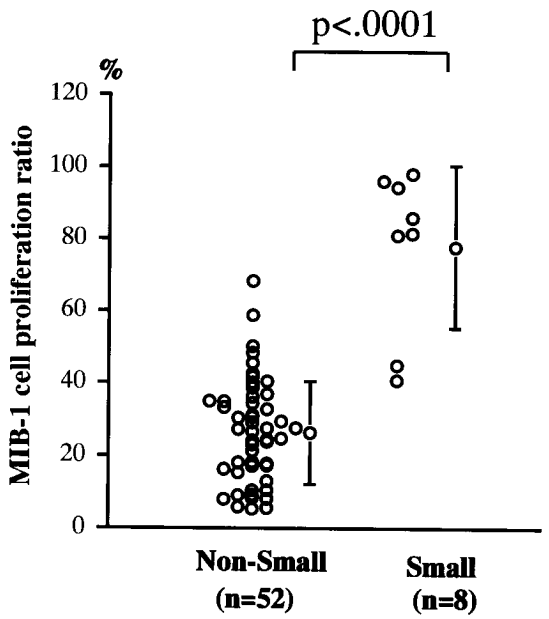


**Fig. 1** MIB-1 cell proliferation ratio in small cell (n = 8) and non-small cell carcinoma (n = 52). There is a highly significant difference between the two values based on an unpaired t-test ($p < 0.0001$).

Two observers (M.I. and K.F.), blinded to the patients' clinical status, independently evaluated the $^{201}$Tl images for the presence of increased uptake in the region of the primary tumor (based on the CT image). Early and delayed $^{201}$Tl images were displayed side-by-side on the computer monitor to detect uptake in the primary lesions. A four-point scale was applied: 0, less than or equal to background activity; 1, possible uptake greater than background; 2, definite, but not intense uptake; 3, definite, clear and intense uptake. Foci of activity that were classified as having an intensity of 2 to 3, and $^{201}$Tl uptake were considered to be tumor. Foci of activity that were classified as 0 to 1 were not. When there was disagreement, the two readers reached a consensus.

Regions of interest (ROIs) were manually drawn over selected areas showing the greatest activity in the tumor, and ROIs were also drawn in a "mirror image" distribution on the contralateral side. The early and delayed $^{201}$Tl index was defined as the ratio of average counts per pixel in the tumor ROIs to those in the contralateral ROIs. The retention index of $^{201}$Tl was calculated for the lung tumor activity according to the following equation[4]: Retention Index (%) = (delayed index − initial index) × 100/initial index. This method assumed a linear rate of tracer clearance and was based on an extrapolation of delayed activity at 3 hours. ROIs were assigned to tumor areas, but not to the mediastinum.

*Surgical and Pathologic Correlation*

Pathologic confirmation of the primary lung lesion was obtained by histopathologic examination of resected

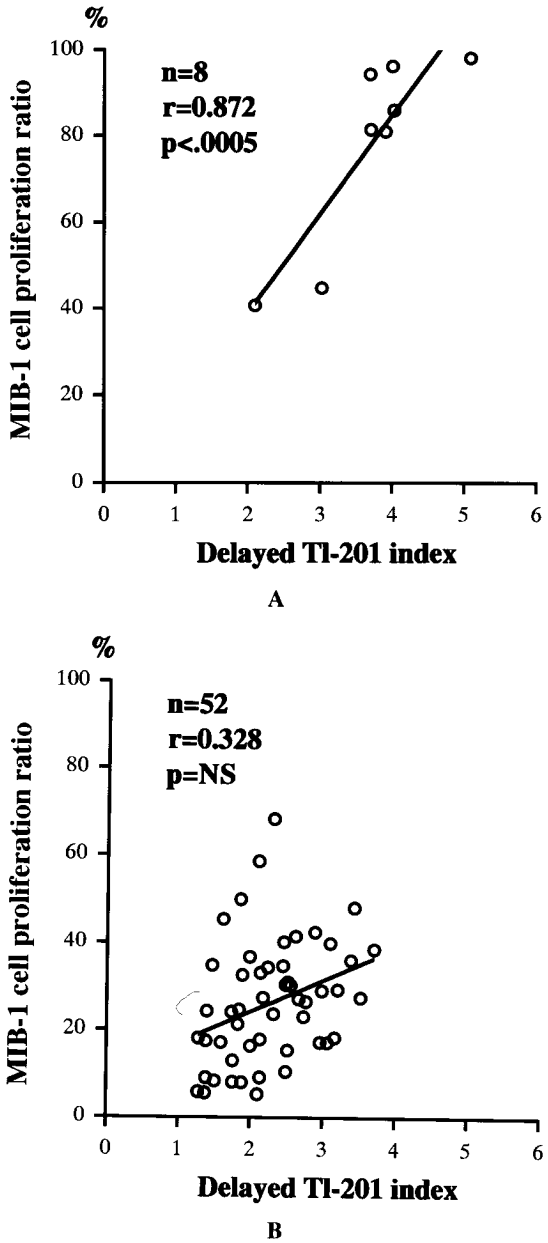


**Fig. 2** 2A, MIB-1 cell proliferation ratio and $^{201}$Tl index on delayed images in small cell lung carcinoma. There is a significant correlation ($r = 0.872$, $p < 0.0005$) between the two values. 2B, MIB-1 cell proliferation ratio and $^{201}$Tl index on delayed images in non-small cell lung carcinoma. There is not a significant correlation ($r = 0.328$, $p = NS$) between the two values.

specimens in 36 of the 60 patients, and by histopathologic examination of biopsy specimens in the remaining 24. Specimens to be evaluated by light microscopy were fixed in 10% formalin for 24 hr, embedded in paraffin, cut into sections 3 $\mu$m thick, and stained with hematoxylin-eosin (H&E). All specimens were also used for immunohistochemical analysis.

*Immnunohistochemical Study*

For immunohistochemical staining, 3 $\mu$m thick slices

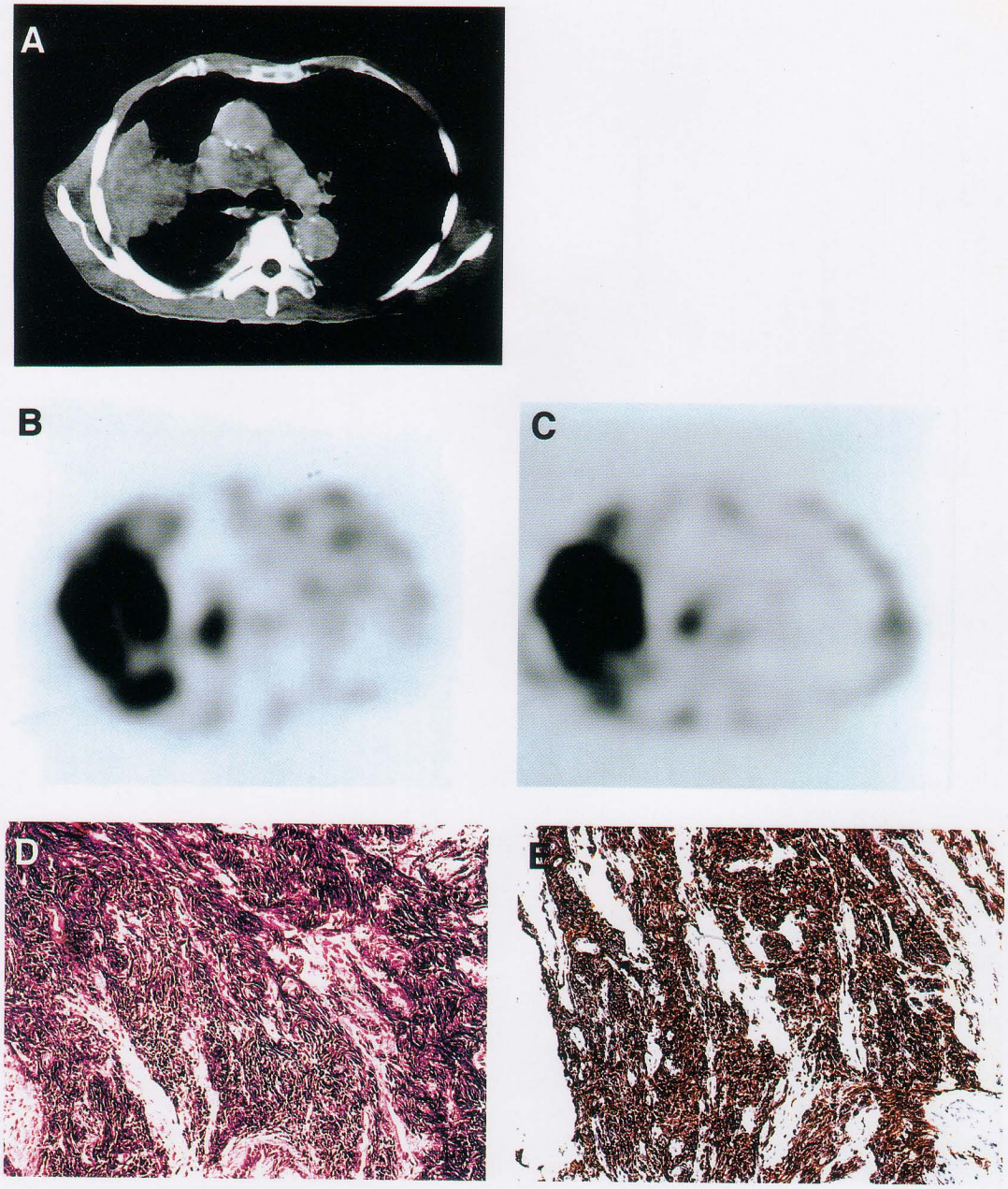


**Fig. 3** A 77-year-old man with a parenchymal nodule in the right lower nodule. (A) Contrast enhanced CT of the chest shows a pulmonary lung lesion. (B and C) Transaxial image from $^{201}$Tl SPECT imaging shows intense uptake in the nodule at 3 hours after radiotracer injection [early (B) and delayed (C) images]. (D) Histopathologic examination of a specimen obtained during fiberoptic bronchoscopy shows the typical features of small cell carcinoma. (H&E, × 50) (E) Immunohistochemical staining of the specimen shows a high-rate of MIB-1 positivity, with the cell proliferation ratio of 98.1% (magnification × 200).

were used. Before staining, all specimens were heated in a 10 mM citrate buffer solution for 15 minutes, in a microwave oven. A commercially-available monoclonal antibody (MIB-1) was used (1 : 50 dilution; Cat. No. 0505, Immunotech S.A., Marseille, France). This antibody reacts with the Ki-67 nuclear antigen associated with cell proliferation and has been found throughout the cell cycle, in $G_1$ to $G_2M$.[11] A DAKO LSAB Kit (DAKO Corp., Carpinteria, CA, USA), based on the labeled streptavidin-biotin (LSAB) method, was used for immunohistochemistry. Endogenous peroxidase activity was blocked by first incubating the specimen for 5 minutes in a methanol solution with 3% hydrogen peroxide. Non-specific staining was blocked by incubation with carrier protein for 5

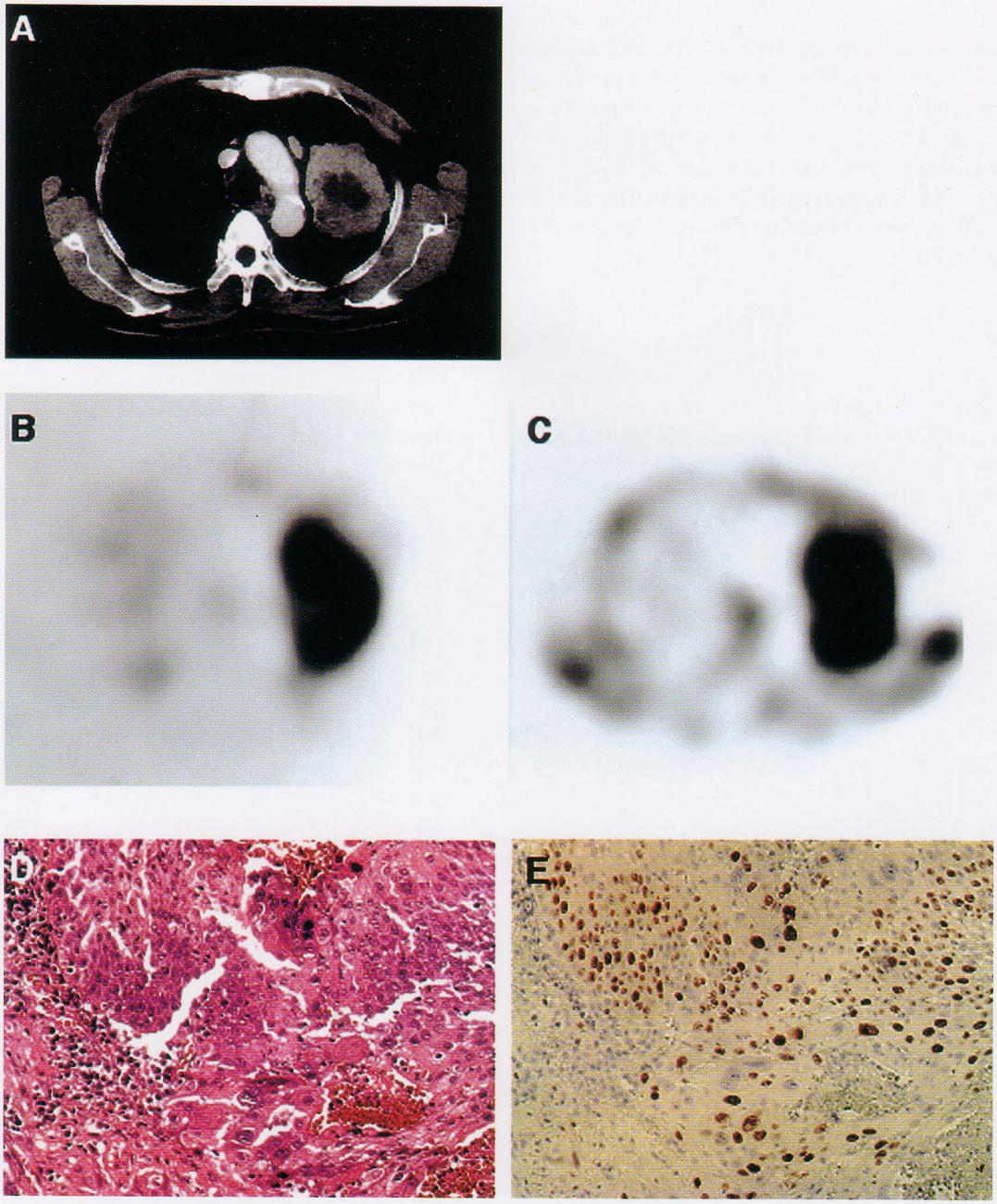


**Fig. 4** A 64-year-old man with lung cancer. (A) Contrast enhanced CT shows a primary lung lesion (24 mm, short-axis dimension). (B and C) Transaixal images from $^{201}$Tl SPECT imaging shows intense uptake by the nodule at 3 hours after radiotracer injection [early (B) and delayed (C) images], but there was no uptake in the mediastinum, in the region of the enlarged node. (D) Histopathologic examination of a specimen obtained during surgically-resected specimen shows typical features of non-small cell carcinoma (squamous cell carcinoma) (H&E, × 50) (E) Immunohistochemical staining of the specimen shows less frequent MIB-1 positivity, with the cell proliferation ratio of 40.3% (magnification × 200).

minutes. The specimens were then incubated with the MIB-1 mAb for 2 hr at room temperature, followed by sequential 10-minute incubations with biotinylated link anti-mouse IgG and peroxidase-labeled streptavidin. Staining was completed after 10 minutes of incubation with substrate-chromogen solution. Staining of the nuclear region in the carcinoma cells was considered a positive result and the MIB-1 cell proliferation ratio was calculated by counting the number of positive cells per 2000 cancer cells in surgically-resected specimens, or per 500 cancer cells in biopsy specimens in a cell counter (OL-501A, Weltech, Kitakyushu, Japan). The cell proliferation ratio was determined by two experienced observers (T.F. and H.Y.) blinded to the patients' clinical status.

*Statistical analysis*

All quantitative data are expressed as the mean ± standard deviation. Comparisons between groups were performed by an unpaired Student's t-test (Statview; Abacus Concepts Inc., Berkeley, CA, USA). A probability level of less than 0.05 was considered significant. Simple linear regression analysis was applied by means of the principle of least squares for evaluation of the cell proliferation ratio and $^{201}$Tl data.

## RESULTS

The $^{201}$Tl images demonstrated uptake > grade 2 in the primary lesions in all patients. On CT scan, these lesions were enhanced with injection of iodinated contrast. Histopathologic diagnoses of the 60 patients' lesions (Table 1) included small cell carcinoma (n = 8) and non-small cell carcinoma (n = 52); the latter included adenocarcinoma (n = 26), squamous cell carcinoma (n = 23), large cell carcinoma (n = 1) and adenosquamous carcinoma (n = 2). The TNM staging system produced Table 2.

The average $^{201}$Tl index of all lung tumors was 2.13 ± 0.61 on early images and 2.46 ± 0.83 on delayed images [retention index (RI) 17.44 ± 35.01%]. In patients with non-small cell carcinoma, the mean $^{201}$Tl index was 2.07 ± 0.62 on early images and 2.28 ± 0.64 on delayed images (RI 13.95 ± 31.92%). In patients with small cell carcinoma, the mean $^{201}$Tl index was 2.58 ± 0.53 on early images and 3.69 ± 0.86 on delayed images (RI 41.21 ± 45.41%) (Table 3). There was a statistically significant difference between the $^{201}$Tl index ($p < 0.005$) on delayed images for non-small cell carcinoma compared with those values for small cell carcinoma. There was a statistically significant difference ($p < 0.0001$) between the cell proliferation ratio for non-small cell carcinoma and that for small cell carcinoma (Fig. 1). There was no correlation ($r = 0.37$, $p < 0.01$) between the $^{201}$Tl index on early images and the cell proliferation ratio, but there was a positive correlation ($r = 0.700$, $p < 0.0001$) between the $^{201}$Tl index on delayed images and the cell proliferation ratio. Of interest, there was a significant correlation ($r = 0.872$, $p < 0.0005$) between the $^{201}$Tl index on delayed images and the cell proliferation ratio in patients with small cell lung carcinoma (Fig. 2A) but not non-small cell lung carcinoma ($r = 0.328$; Fig. 2B). There was no correlation ($r = 0.307$, $p < 0.01$) between the RI and the cell proliferation ratio.

Representative CT and $^{201}$Tl SPECT images are shown in Figures 3 and 4. Figure 3 shows a pulmonary nodule with intense $^{201}$Tl uptake (Figs. 3B and 3C). Histopathologic evaluation of a biopsy specimen confirmed small cell carcinoma (Fig. 3D). The cell proliferation ratio for this patient was 98.1% (Fig. 3E). By contrast, in Figure 4, a primary lung lesion on CT scan (Fig. 4A) demonstrated increased $^{201}$Tl uptake on $^{201}$Tl SPECT (Figs. 4B and 4C) and was found to be non-small cell carcinoma (squamous cell carcinoma) (Fig. 4D). The cell proliferation ratio for this patient was 40.3% (Fig. 4E).

## DISCUSSION

This study suggests that $^{201}$Tl uptake in small cell but not non-small cell lung carcinoma correlates with cell proliferation although CT provides all the information one needs. Our data suggest that the most important relationship is between $^{201}$Tl and the cell proliferation ratio. Since tumor cell proliferation is closely associated with the malignant potential, this may be a means of assessing the biologic behavior of tumors, or for selecting subgroups of patients for alternative therapies. The initial description of lung tumor uptake of $^{201}$Tl was made in 1976 by Cox et al.,[1] who reported $^{201}$Tl uptake in a patient with primary bronchial carcinoma. Tonami and colleagues[4] have described the retention index, an indicator of the degree of $^{201}$Tl retention in the lesion, and have shown that this index is useful in differentiating between malignant and benign lesions, possibly reflecting the intensity of Na-K ATPase expression determined by immunohistochemical staining as previously described by Takekawa et al.[17]

Several researchers have described the mechanism of uptake and retention of $^{201}$Tl in tumors.[5–10,14] Brismar et al.[6] reported that the high specific $K^+$ and $Tl^+$ accumulation in cultured human glioma cells was due not to the presence of inwardly rectifying $K^+$ channels or other identified $K^+$ channels, but to Na,K-ATPase dependent transport and Na-K-Cl cotransport. Ishibashi et al.[14] have reported that uptake of $^{201}$Tl in glioma may reflect the cell proliferation detected with the proliferating cell nuclear antigen (PCNA) and Ki-67 monoclonal antibody.

Clinical assessment of the response to therapy is a major problem in the follow-up and management of patients with lung cancer. Ki-67 and MIB-1 monoclonal antibodies have been reported to be good markers of proliferative activity in a variety of tumors.[18–20] $^{201}$Tl imaging may play a role in assessing the effect of treatment because the $^{201}$Tl index on delayed images was significantly correlated with the number of small cell lung carcinoma patients with the degree of cancer cell proliferation reflected in by the cell proliferation ratio although there was no significant correlation between the $^{201}$Tl index on early images, or the retention index and the cell proliferation ratio.

Immunocytochemical investigation by means of flow cytometry has demonstrated that the antigen recognized by the MIB-1 antibody is closely associated with the cell nuclear Ki-67 antigen.[11] Ki-67 antigen expression starts in the S-phase, and progressively increases through the S- and $G_2$-phase, reaching its maximum at mitosis. After division, the cells return to the $G_1$-phase with a stock of Ki-67 antigen. The Ki-67 level decreases progressively during this phase and finally disappears in cells with a long $G_2$-phase.[21,22] In our study $^{201}$Tl indices in lung

cancer were compared to the degree of cell proliferation in tumor specimens by using MIB-1 mAb, and we found that the delayed $^{201}$Tl index was closely correlated with the tumor cell proliferation of small cell lung carcinoma. In the tumors studied, there was a relatively homogeneous distribution of MIB-1 positive cells, with no areas of frank necrosis; therefore, counting and averaging of a number of fields appeared to provide an accurate measurement of the labeling index. Tungekar et al.[23] reported that measurement of the lung tumor growth rate with Ki-67 mAb showed promise as an indicator of short-term survival and perhaps as a means of selecting patients with adenocarcinoma and squamous cell carcinoma for postoperative chemotherapy. Furthermore, our data show that there was significant difference ($p < 0.0001$) between non-small cell and small cell lung cancer in the cell proliferation ratio. Clinical assessment of the response to therapy is a major problem in the follow-up of patients with lung cancer. Nevertheless, treatment is not very good, and further study is warranted to determine whether this is an independent prognostic marker for this cancer. To do this we need to devise another study in which $^{201}$Tl is correlated with survival data.

In conclusion, we found a good correlation between the delayed $^{201}$Tl index and the cell proliferation ratio in patients with small cell but not non-small cell lung carcinoma. To the extent that $^{201}$Tl imaging can provide this information about the entire tumor, radionuclide imaging may provide an important prognostic information.

## ACKNOWLEDGMENT

The authors are grateful to H. William Strauss, M.D. (Stanford University School of Medicine, Palo Alto, CA) for his valuable suggestions and contributions to this study.

## REFERENCES

1. Cox PH, Belfer AJ, Pompe WB. Thallium-201 chloride uptake in tumors, a possible complication in heart scintigraphy. *Br J Radiol* 16: 425–430, 1976.
2. Salvatore M, Carratu L, Porta E. Thallium-201 as a positive indicator for lung neoplasm: preliminary experiments. *Radiology* 121: 487–488, 1976.
3. Tonami N, Hisada K. Clinical experience of tumor imaging with Tl-201 chloride. *Clin Nucl Med* 2: 75–81, 1977.
4. Tonami N, Shuke N, Yokoyama K, et al. Tl-201 single photon emission computed tomography in the evaluation of suspected lung cancer. *J Nucl Med* 30: 997–1004, 1989.
5. Takekawa H, Itoh K, Abe S, et al. Retention index of thallium-201 single photon emission computerized tomography (SPECT) as an indicator of metastasis in adenocarcinoma of the lung. *Br J Cancer* 70: 315–318, 1994.
6. Brismar T, Anderson S, Collins VP. Mechanism of high $K^+$ and $Tl^+$ uptake in cultured human glioma cells. *Cell Mol Neurobiol* 15: 351–360, 1995.
7. Brismar T, Gruber A, Peterson C. Increased cation transport in *mdr*1-gene-expressing K562 cells. *Cancer Chemother Pharmacol* 36: 87–90, 1995.
8. Ballinger JR, Sheldon KM, Boxen I, Erlichman C, Ling V. Differences between accumulation of $^{99m}$Tc-MIBI and $^{201}$Tl-thallous chloride in tumour cells: role of P-glycoprotein. *Q J Nucl Med* 39: 122–128, 1995.
9. Brismar T, Collins VP, Kesselberg M. Thallium-201 uptake relates to membrane potential and potassium permeability in human glioma cells. *Brain Research* 500: 30–36, 1989.
10. Sessler MJ, Geck P, Maul FD, Hor G, Munz DL. New aspects of cellular thallium uptake: $Tl^+$-$Na^+$-2Cl(−)-cotransport is the central mechanism of ion uptake. *Nuklearmedizin* 25: 24–27, 1986.
11. Cattoretti G, Becker MHG, Key G, Firby P, Hartman NG, Moore MJ. Monoclonal antibodies against recombinant parts of the Ki-67 antigen (MIB1 and MIB3) detect proliferating cells in microwave-processed formalin-fixed paraffin sections. *J Pathol* 168: 357–363, 1992.
12. Youssef EM, Matsuda T, Takada N, et al. Prognostic significance of the MIB-1 proliferation index for patients with squamous cell carcinoma of the esophagus. *Cancer* 76: 358–366, 1995.
13. Lee CS. Difference in cell proliferation and prognostic significance of proliferating cell nuclear antigen and Ki-67 antigen immunoreactivity *in situ* and invasive carcinoma of the extrahepatic biliary tract. *Cancer* 78: 1881–1887, 1996.
14. Ishibashi M, Taguchi A, Sugita Y, et al. Thallium-201 in brain tumors: the relationship between the tumor cell activity in astrocytic tumor and proliferating cell nuclear antigen (PCNA). *J Nucl Med* 36: 2201–2206, 1995.
15. American Thoracic Society. Medical section of the American Lung Association: clinical staging of primary lung cancer. *Am Rev Respir Dis* 127: 659–664, 1983.
16. Beahrs OH. Manual for staging of cancer, 4th ed. American Joint Committee on Cancer (AJCC), Philadelphia, JB Lippincott, pp. 115–122, 1992.
17. Takekawa H, Itoh K, Abe S, et al. Thallium-201 uptake, histological difference and Na-K ATPase in lung adenocarcinoma. *J Nucl Med* 37: 955–958, 1996.
18. Price P, Bush C, Parkinson CS, Imrie P, Ormerod MG, Steel CG. Ki-67 in the assessment of tumor growth rate: a study on xenografts. *Int J Radiat Biol* 56: 787–800, 1989.
19. Nielssen AL, Nyholm HC, Engel P. Expression of MIB-1 (paraffin Ki-67) and AgNCR morphology in endometrial adenocarcinomas of endometrioid type. *Int J Gynecol Pathol* 13: 37–44, 1994.
20. Simony J, Pujol JL, Radal M, Ursule E, Michel FB, Pujol H. *In situ* evaluation of growth fraction determined by monoclonal antibody Ki-67 and ploidy in surgically resected non-small cell lung cancers. *Cancer Res* 50: 4382–4387, 1990.
21. Lopez P, Belloe F, Lacombe F, et al. Modalities of synthesis of Ki-67 antigen during the stimulation of lymphocytes. *Cytometry* 12: 42–49, 1991.
22. Buruno S, Darzynkiewiez Z. Cell cycle dependent expression and stability of the nuclear protein detected by Ki-67 antibody in SHL-60 cells. *Cell Prolif* 25: 31–40, 1992.
23. Tungekar MF, Gatter KC, Dunnil MS, Mason DY. Ki-67 immunostaining and survival in operable lung cancer. *Histopathology* 19: 545–550, 1991.